Genetic regulators of mineral amount in Nelore cattle muscle predicted by a new co-expression and regulatory impact factor approach

Juliana Afonso[1], Marina Rufino Salinas Fortes[2], Antonio Reverter[3], Wellison Jarles da Silva Diniz[1], Aline Silva Mello Cesar[4], Andressa Oliveira de Lima[1], Juliana Petrini[5], Marcela M. de Souza[6], Luiz Lehmann Coutinho[7], Gerson Barreto Mourão[4], Adhemar Zerlotini[8], Caio Fernando Gromboni[9], Ana Rita Araújo Nogueira[10], Luciana Correia de Almeida Regitano[*10]

[1]Department of Evolutionary Genetics and Molecular Biology, Federal University of São Carlos, São Carlos, Brazil, [2]School of Chemistry and Molecular Biosciences, Faculty of Sciences, The University of Queensland, Brisbane, Australia, [3]Agriculture and Food, Commonwealth Scientific and Industrial Research Organisation, Brisbane, Australia, [4]Department of Agroindustry, Food and Nutrition, University of São Paulo/ESALQ, Piracicaba, Brazil, [5]Department of Statistics, Institute of Exact Sciences, Federal University of Alfenas, Alfenas, Brazil, [6]Department of Animal Science, Iowa State University, Ames, IA, USA, [7]Department of Animal Science, University of São Paulo/ESALQ, Piracicaba, Brazil, [8]Bioinformatic Multi-user Laboratory, Embrapa Informática Agropecuária, Campinas, São Paulo, Brazil.[9] Bahia Federal Institute of Education, Science and Technology, Ilhéus, Brazil,[10]Embrapa Pecuária Sudeste, São Carlos, Brazil, [*]Corresponding author.

**Correspondence to: luciana.regitano@embrapa.br*

Abstract

Mineral amount in bovine muscle affect meat quality, growth, health and reproductive traits in beef cattle. To better understand the genetic basis of this phenotype, we implemented new applications of use for two complementary algorithms: the partial correlation and information theory (PCIT) and the regulatory impact factor (RIF), by including GEBVs as part of the input. We used PCIT to determine putative regulatory relationships based on significant associations between gene expression and mineral amount. Then, RIF was used to determine the regulatory impact of genes and miRNA expression over mineral amount. We also investigated over-represented pathways, as well as evidences from previous studies carried in the same population, to determine regulatory genes for mineral amount *e.g. NOX1*, whose expression was positively correlated to Zn and was described as regulated by this mineral in humans. With this methodology, we were able to identify genes, miRNAs and pathways not yet described as important for mineral amount. The results support the hypothesis that extracellular matrix interactions are the core regulator of mineral amount in muscle cells. Putative regulators described here add information to this hypothesis, expanding the molecular relationships between gene expression and minerals.

Keywords: Nelore, minerals, genes, miRNA, PCIT, RIF.

Introduction

Mineral amount affects meat quality [1]–[4], reproduction [5], health and growth performance [6], [7] in beef cattle and the control of mineral homeostasis depends on genetic factors, among others [8]. Understanding the genetic aspects linked to mineral amount in bovine muscle can lead to a better modulation of this trait, allowing for future production of healthier, more productive animals, and better-quality meat.

A differential expression approach detects genes and pathways underlying mineral amount in Nelore cattle, by comparing extremes of the population used herein [9] [10]. However, as mineral amount traits occur in a continuous distribution, to verify these relationships and infer regulatory modes of action, it is necessary to study the whole population. It is possible to go beyond contrasting extreme phenotypes, beyond differential expression [11]. Thus, by applying a co-expression network approach it is possible to identify genome-wide genes with similar expression patterns related to specific phenotypes or conditions. In this methodology, traits are usually integrated into the analysis in a condition-dependent network, by previous selection of genes or sample clusters related to the trait before the analysis [12]. Another way of including phenotypes to select gene groups putatively involved with them, already used for mineral amount in our population [13], is to cluster all expressed genes by their co-expression profiles and then associate these clusters to the phenotypes using the Weighted correlation network analysis (WGCNA) iR package [14]. In this case, groups of genes with similar functions are identified and associated with the phenotypes.

Among the challenges of these methods regarding phenotype inclusion is that no single approach is used to search genome-wide for specific genes linked to phenotypes without prior selection. Also, it is challenging to pinpoint the direction of interactions or the regulation, as co-expression networks do not provide this information a priori [12]. To overcome these limitations, we propose a new application of the partial correlation and information theory (PCIT) algorithm, originally used for deriving gene co-expression networks, by identifying significant associations between expression profiles [15]. Additionally, we propose a new application of the regulatory impact factor (RIF) algorithm [16] to identify significant genes and miRNAs expression with regulatory impact over mineral amount in bovine muscle. To this end, we used the expression values of genes and miRNAs correlated to minerals instead of transcription factors (TFs) used in the original application, allowing the regulatory role to go beyond current functional annotation of the

cattle genome. When calculating the RIF of genes and miRNAs with expression correlated with a mineral over the amount of this mineral, the mineral mass fraction genomic estimates of breeding values (GEBVs) were used instead of the expression data of selected gene. Therefore, we were able to use GEBVs on the networks to identify regulatory elements linked to the phenotypes. This new use of the PCIT-RIF algorithms identified genes and miRNAs expression related to the mass fraction of calcium (Ca), copper (Cu), potassium (K), magnesium (Mg), sodium (Na), phosphorus (P), sulfur (S), selenium (Se), zinc (Zn) and iron (Fe) in Nelore steers' *Longissimus thoracis* muscle. In short, we aimed to predict the regulatory impact of genes and miRNAs expression over mineral amount in Nelore muscle.

Results

Genes and miRNAs with expression values correlated to minerals

After data quality control, filtering, normalization and batch effect correction performed separately in the mRNA-Seq and miRNA-Seq from 113 samples, the expression of 12,943 genes and 705 miRNAs remained for further analyses. To identify genes and miRNAs with expression values correlated to ten different minerals, we carried out two different PCIT analyses, using our new application: i) PCIT general: incorporating genes, miRNAs expression and GEBVs together, and ii) PCIT miRNA: considering only miRNAs expression and GEBVs together. Simultaneously considering the results of both PCIT analyses, we identified a total of 242 genes and 35 miRNAs with expression values correlated to at least one mineral GEBV. From these, the expression of 46 genes and 12 miRNAs was correlated to more than one mineral GEBV. The number of genes and miRNAs with expression values correlated to each mineral ranged from 19 to 55 and from five to nine, respectively. The number of miRNAs' expression that were correlated to a mineral in both PCIT analyses varies from zero to three (Table 1). There were two genes and one miRNA expression values correlated to six minerals, Vitamin D3 receptor (*VDR)* and bta-miR-92b correlated to Ca, K, Mg, Na, P and S; and Doublecortin (*DCX)*, correlated to K, Mg, Na, P, S, and Zn. From these analyses, we identified significant correlations among minerals' GEBVs. There were no significant correlations between Se and other minerals (Figure 1). Correlations identified among K, Mg, Na, Zn, S, and P GEBVs ranged from 0.77 to 0.97.

Principal component score and Regulatory Impact Factor (RIF)

From a principal component analysis based on the GEBVs for each animal, considering ten minerals, we calculated a score for each sample regarding its contribution to phenotypic variation. Based on that, we selected 30 contrasting samples concerning all minerals together, 15 with low score and 15 with high score (Figure 2). These contrasting groups were used to estimate the RIF of all genes and miRNAs with expression values correlated to at least one mineral in the amount of all minerals together, using our application of the original RIF algorithm (see methods). Also, we estimated the RIF of the genes and miRNAs with expression values correlated to each mineral separately using contrasting sample groups for specific minerals. For that, based on the GEBVs, we expanded to 15 the number of samples on the same contrasting groups detailed in previous works with differentially expressed genes regarding mineral amount [9] [10] containing six samples for Ca, Cu, K, Mg, Na, P, S, Se and Zn and five samples for Fe in each group.

There were 22 genes and two miRNAs with significant RIF based on the high and low score approach. Based on the single mineral analysis, there were three common genes and one common miRNA with significant RIF for two minerals, CD86 molecule (*CD86)* for K and Mg, *VDR* for Mg and Na, WD repeat-containing planar cell polarity effector (*WDPCP)* for Na and P and bta-miR-369.3p for Ca and S. The number of genes with significant RIFs for each mineral varied from zero to seven and for miRNA from zero to two (Table 2). The RIF values of each gene and miRNA presenting significant RIF for each mineral and score analysis is in Supplementary Table S1.

Correlation network

We used the significant correlations between a gene or a miRNA expression and a given mineral, identified in both analyses implemented with the PCIT algorithm, as above described, to derive a co-expression correlation network. To identify potential regulatory mechanisms related to each mineral, we added on this network other layers of information from the same samples, tissue and population, as follows: differentially expressed genes (DEGs) for contrasting mineral amount sample groups [9] [10], transcription factors (TF) [17] and genes affected by eQTLs [18]. This information and genes with significant RIFs were used as node attributes and included in the network analyses (Figure 1). All correlations and attributes necessary to compose Figure 1 are provided (see Supplementary Table S2).

There was at least one putative regulatory element (*i.e.* a significant RIF, TF, miRNA, or gene affected by eQTLs) correlated to each mineral. The number of genes and miRNAs with expression values correlated per mineral per attribute identified is showed in Table 3 and the genes, miRNAs and their attributes are showed in Supplementary Table S2.

There were no functional clusters or over-represented pathways identified in the functional annotation analysis carried out separately for each group of genes correlated to a specific mineral. However, from the functional annotation table, we noted that the gene expressions correlated to the minerals are well conserved among a broad range of organisms. They have functions related to the extracellular matrix, integral membrane constituents, metal ion binding, and partake on regulatory processes linked to transcription, replication, splicing, apoptotic processes, metabolism, transport vesicles, RNA processing, signaling, cell division, adhesion, migration and proliferation, embryonic development and tissue regeneration.

Integration with differentially expressed genes (DEGs)

To convey the relationship among all genetic elements related to mineral mass fraction detected in our population, we used PCIT to estimate the correlations between a gene or miRNA expression that was found to be correlated to a given mineral in the present work and DEGs previously identified for the same mineral [9] [10]. This analysis was carried out for each mineral separately and included the same genes with regulatory potential as in the previous section (DEGs [9] [10], TFs [17], genes affected by eQTLs [18] and genes with significant RIF). To identify elements with regulatory potential, we then selected the genes that were network hubs or that were significant according to RIF (see methods). We performed a functional annotation analysis with the selected genes for each mineral, separately, to determine which ones were underlying biological pathways.

The expression of all selected putative regulatory elements (hub, significant RIF or miRNA), the ones underlying biological pathways newly identified and the ones being part of enriched pathways in previous work with DEGs related to mineral amount [9] [10] were used as inputs for a final PCIT analyses. This PCIT was carried to identify possible regulators of genes in enriched pathways. Figure 3 shows the co-expression networks built with significant correlations from the final PCIT analyses for Ca, Cu, K, Mg, Na, P, S, Se, and Fe. Supplementary Tables S3 has the correlations and attributes related to creating Figure 3.

As we included the differentially expressed genes regarding mineral amount previously detected in in the same population [9] [10], most of the over-represented pathways

identified correspond to the previously detected pathways expression analyses. In addition, by the inclusion of correlated genes and pathways from the Reactome database [19], we identified new pathways for K, related to protein metabolism, for Ca, Cu, S and Fe related to immune response, and for S related to signaling. All the pathways enriched for S are new, when compared with our previous work [9]. A list of the pathways enriched for each mineral considering the ones detected with the inclusion of correlated genes expressions and the ones from the previous work [9] [10] is shown in Table 4.

Regarding Zn, no gene taking part in the unique enriched pathway previously detected [9] met our criteria. Because of that, for this mineral, we generated a co-expression network by including the DEGs for Zn [9] that had their expression values significantly correlated to hub or RIF elements for Zn and their attributes, in order to identify possible regulators for the DEGs in general. This co-expression network is shown in Figure 4, and the correlations and attributes supporting Figure 4 are presented in Supplementary Table S4.

Discussion

Relationship among minerals

Correlations identified among GEBVs for most minerals were high (0.77 to 0.97). Thus, a word of caution must inform this discussion of all genes and miRNAs with expression values correlated to each mineral, as correlated responses across minerals may underlie the identified genes and miRNAs, as well as their predicted relationships. All minerals, except Se, were correlated among themselves and all of them revealed genes in common, in the correlation network. In this network, the link between Se and the other minerals was Zn, through the common correlation with the NADPH oxidase 1 (*NOX1)* gene expression, which had significant RIF results for Zn. *NOX1* expression was positively correlated to Zn and negatively to Se. Accordingly, Zn positively regulates NOX1 protein expression in humans, since an increase in Zn leads to a Zn accumulation in the mitochondria. This accumulation increases the production of reactive oxygen species which activates NF-Kb, a known positive transcriptional regulator of *NOX1*, thus increasing its expression [20]. Moreover, Se deficiency is known to induce the oxidation of NrX, a transmembrane protein, by the accumulation of H_2O_2, which is catalyzed by the NOX1 protein [21]. As the Se deficiency and the H_2O_2 accumulation catalyzed by the NOX1 protein act in the same known biochemical process, this could explain the negative

correlation found in our analysis. Further, the oxidation of NrX protein leads to the activation of the Wnt signaling pathway [21], that can act in adult muscle regeneration [22], an evidence for the relevance of this regulation for muscle homeostasis. Another link between Se and Zn were the correlations with three miRNAs expressions: bta-miR-411c-5p (with significant RIF for Zn), bta-miR-2285co and bta-miR-2285bl, although no literature relates these miRNAs to Se or Zn amount, nor to the genes related to these minerals in our analysis.

Fe exhibited a weak correlation with Mg, K, P, and S (from 0.25 to 0.31, $p < 0.05$) and was linked to other minerals through S, sharing negative correlations with the expression of 1-phosphatidylinositol 4,5-bisphosphate phosphodiesterase gene (*PLCB2)*. PLCB2 protein is critical to Ca efflux [23], although no correlation with Ca amount was found in our data, nor in our previously reported DEGs [9]. The relationship of *PLCB2* gene expression with Fe and S is undocumented, although Fe was reported to cleave the PLCB2 protein in the cornea of bovine, porcine and humans [24]. The *PLCB2* gene is affected by 61 trans eQTLs, harbored across 12 chromossomes [18], making these eQTL regions candidates to regulate this gene expression and consequently Fe and S mass fractions in the muscle.

PCA score analyses identified regulators of mineral composition

Our score successfully detected contrasting samples regarding all minerals together, allowing for the identification of genes and miRNAs with significant overall RIFs. Considering these genes and the functional enrichment analysis, we identified well-conserved functions for 14 out of 22 genes. From these, we can highlight three with functions related to minerals: Delta-aminolaevulinic acid dehydratase (*ALAD)* encodes a metal ion binding protein linked to Zn, Zinc finger CCHC domains-containing protein 7 (*ZCCHC7)*, which encodes a chaperone and Zn finger protein, while Myosin light chain kinase 3 (*MYLK3)* is part of the Ca signaling pathway that participates in muscle contraction.

Mutations in the *ALAD* gene were linked to the phenotypic expression of potentially toxic metal by fly ash exposure in cattle born near thermal power plants, being pointed as a candidate for genomic studies related to metal toxicity [25]. Our results indicated that *ALAD* is a candidate linked to minerals in general, including potentially toxic metals.

Functional analyses and the search of regulatory elements

Functional annotation analyses, performed based on the genes with expression values correlated to each mineral, showed no functional clusters nor enriched pathways for any mineral. However, some of these genes' expressions were correlated with DEGs partaking in different pathways and are themselves part of these pathways, which lead us to hypothesize that the remaining genes of the pathways may be modulated in less intensity. This agrees with the small QTL effects already observed for mineral amount [26]. The function annotation for each gene separately showed membrane proteins and extracellular matrix (ECM) related proteins as common annotation for many genes. This observation helps to corroborate the hypothesis that ECM interactions are at the regulatory core for the mineral mass fraction [9]. ECM pathways were enriched for co-expressed groups of genes related to mineral mass fraction and meat quality traits in this Nelore population [13].

When components of a specific pathway are known, a guided-gene approach in a co-expression network can help to identify new genes for the same pathway-related-trait [27], and a pre-selection of genes by biological meaning can improve the network interpretation [12]. Our selection based on enriched pathways, TFs, and significant RIF allowed the inference of genes and miRNAs with a regulatory potential in these pathways. We identified high correlations among these selected elements when compared with the correlations among unselected genes/miRNAs and minerals or considering all genes/miRNAs correlated to a mineral and their respective DEGs. These high correlations and the presence of genes related to regulatory processes reinforces that our methodology can be used to drive the search for meaningful regulatory relationships.

Potential regulators for more than one mineral

Genes with significant RIF and genes with expression values correlated to others that belong to enriched pathways are the potential regulators. These candidate genes may modulate mineral mass fraction by affecting their target genes and pathways. For the minerals presenting enriched pathways, except Zn, the elements with significant RIFs were connected with miRNAs, correlated genes expressions, TFs and genes being affected by trans eQTLs. They were also part of enriched pathways, reinforcing their regulatory role on the phenotypes. The intricate patterns obtained in these network analyses arise from the fact that the same genes are part of different pathways.

As expected, the pathways identified by considering gene expression correlation with mineral GEBVs were often the same already reported in the differential expression study [9]. The pathways with functions related to ECM processes and protein metabolism were enriched for almost all minerals, except Se, Fe, and Zn. These results also corroborate our previous hypothesis that the regulatory core of mineral amount is linked to ECM processes [9]. Pathways related to fatty acid metabolism were enriched for Cu, as reported in that previous study. However, with the inclusion of the genes with expression values correlated to the minerals, pathways linked to immune responses were enriched for Ca, Cu, Fe, and S. The pathways enriched for S, related to signal transduction and immune response, were not detected in the previous cited work, emphasizing that the integrative approach used herein can bring up new evidences of regulatory processes not identified under the differential expression analysis.

We identified putative regulators that might impact more than one mineral. Cluster of differentiation 86 gene (*CD86)* showed a significant RIF and was a hub gene for Mg and K analyses. The gene *CD86* encodes a protein signaling for T cell activation and proliferation [28] and is linked to T cell adhesion after activation [29]. A Mg sensor, ITK, seems to be required for optimal T cell activation [30] and K^+ channels are involved in T cell activation, after the binding of the CD86 protein in the CD28 receptor [31], putatively explaining the relationship among these two minerals and *CD86*. The PI3k-akt signaling pathway is activated after this protein-receptor binding in an antigen-presenting cell, leading to downregulation of integrins, participants of the pathways enriched for these two minerals [32]. For both minerals, Mg and K, the known roles of *CD86* support the idea that this is a regulator for the enriched pathways.

The Vitamin D receptor (*VDR*), is a TF with significant RIF for Mg and Na. *VDR* expression has a known relationship with Ca metabolism [33], and it was correlated to this mineral, but it was not identified here as a putative regulator for Ca based on the RIF score. Mg is essential to vitamin D activation, once both enzymes involved in this process, 25-hydroxylase and 1α-hydroxylase, are Mg-dependent [34]. *VDR* expression link with Na is not extensively documented. A putative role of this encoded receptor in the increased Ca absorption and/or reduced Ca loss in menopause women containing no f alleles of the *VDR* gene under a Na and protein-rich diet was reported [35]. The relationship between this gene expression and the ECM processes-related pathways enriched for both minerals seems to be the interaction of the VDR receptor with the Runx2 receptor which, in mammals, stabilizes chromatin remodelers by activating genes involved in ECM mineralization [36].

313 WD repeat-containing planar cell polarity effector (*WDPCP)* is a gene with
314 significant RIF for Na and P and was affected by one trans eQTL in chromosome five [18].
315 The *WDPCP* gene encodes a protein that inhibits Wnt activity [37], whose pathway acts in
316 adult muscle regeneration [22], and is activated by high P amounts [38]. ECM processes-
317 related pathways were also enriched for these minerals. ECM stiffness increases the
318 expression of several members of the Wnt pathway through integrins and focal adhesion
319 pathways [39], thus relating the *WDPCP* gene expression with the enriched pathways. The
320 link between *WDPCP* expression and Na is not known. In both minerals, Na and P, *WDPCP*
321 expression value is correlated positively (0.19) with the TF *VDR* expression that represses the
322 Wnt pathway [40].
323 The miRNA bta-miR-369-3p had a significant RIF for Ca and S. The genes with
324 expression values correlated to this miRNA are not known targets to it. This miRNA
325 expression levels increases in skin and serum of humans with psoriasis [41]. A homolog of
326 psoriasin, a common protein in psoriasis patients, was identified in bovines and have the
327 same antimicrobial and immune response activity as the human one [42]. Psoriasis trigger
328 seems to be the activation of the cellular immune system [43], probably explaining why the
329 bta-miR-369-3p expression level was correlated to several genes involved in immune
330 pathways for Ca and S. Further, Ca and vitamin D play important roles in keratinocyte
331 differentiation and regulate proteins involved in psoriasis [44] and S is used as a known
332 treatment and prevention of recurrence for this disease [45]. Our results suggest the genes
333 expressions correlated to bta-miR-369-3p expression as non-described candidate targets of
334 this miRNA, linked to immune response and mineral concentration.
335
336 *Potential regulators for a specific mineral concentration*
337
338 Some putative regulators showed significant RIF for only one mineral. The miRNA
339 bta-let-7i showed significant RIF for Mg and one of the correlated genes, Collagen alpha-1
340 (XI) chain (*COL11A1)* is a target of this miRNA. The *COL11A1* gene is a DEG, associated to
341 protein digestion and absorption, as well as, to ECM receptor interaction. This gene encodes
342 a collagen protein, the most abundant protein in ECM. *COL11A1* expression is correlated to
343 Mg, which stimulates collagen synthesis [46], and its expression is correlated to other genes
344 expressions being part of the same or related pathways. Cystathionine gamma-lyase (*CTH)* is
345 also a gene with significant RIF just for Mg. This gene expression is correlated to a Zn finger

346 protein of the cerebellum (*ZIC3)*, a TF, which was correlated to the already mentioned *CD86*
347 gene expression, also associated with Mg herein.
348 We identified two genes with significant RIF specifically for K: Matrix
349 metallopeptidase (*MMP16)* and E3 ubiquitin-protein ligase (*RNF34)*. The gene *MMP16*
350 encodes a protein whose family is involved in the breakdown of ECM, mostly of collagen
351 genes [47], explaining its link to the enriched pathways related to ECM organization and its
352 correlation with Collagen type XXI alpha 1 chain (*COL21A1)*. Both *MMP16* and *RNF34*
353 expressions were correlated to *CD86* expression, for which the link to K was already
354 discussed. *RNF34* encodes a RINF finger protein that negatively regulates the NOD1
355 pathway, involved in receptors activating immune responses, similar to *CD86*. Bta-miR-92b
356 expression was correlated to seven genes expressions, and one of them, *MMP16*, is a known
357 target for this miRNA regulation, which could explain the relationship of this miRNA with
358 the over-represented pathways.
359 For Na, we identified six genes with significant RIF: *WDPCP* and *VDR*, linked to the
360 already discussed ECM processes, Vimentin type intermediate filament associated coiled-coil
361 protein (*VMAC)*, Cyclin-dependent kinase inhibitor 3 (*CDKN3)*, Centromere protein E
362 (*CENPE)*, and Calcium/calmodulin-dependent protein kinase kinase 1 (*CAMKK1)*. VMAC
363 intermediates filament, play an important role in cytoskeletal organization [48]. Cell
364 adhesions, mediated by integrins, link ECM and cytoskeleton [49]. *CDKN3* encodes a
365 cycling-dependent kinase inhibitor that is involved in cell cycle regulation [50], a process
366 where integrins act [51]. The presence of an integrin gene, integrin subunit alpha 10
367 (*ITGA10)* in the network, as well as actin interactions, could explain the link of these two
368 genes and the ECM-related pathways for Na. Na presents a miRNA with significant RIF, bta-
369 miR-125a, presenting its expression values correlated to two genes with significant RIF,
370 *WDPCP* and *VMAC*, and the integrin gene *ITGA10*. This miRNA targets *VMAC* who is also
371 affected by six trans eQTLs in chromosome six, being candidates to future studies.
372 The miRNAs bta-miR-25 and bta-miR-378c had significant RIF for Fe. Their
373 expression values were correlated to each other, to other miRNAs expression and, as with
374 other miRNA found in our results, the genes expressions correlated to them were not
375 described as their targets. Both miRNAs expressions were correlated to *ALAD* gene
376 expression, also a hub gene in the Fe network. Fe amount in the extracellular environment
377 positively affects ALAD protein level and activity [52]. The relationship with the immune
378 response pathways enriched for Fe seems to be in the proteasome involvement in these

pathways. ALAD protein modulates proteasome activity [53], and proteasome function can shape innate and adaptative immune responses [54].

Lysophosphatidic acid receptor 4 (*LPAR4)* is a hub gene with significant RIF for Ca, already known to positively regulate cytosolic Ca amount involved in phospholipase C-activating G protein-coupled signaling pathway (GO:0051482). Its expression is linked in our network to MAF BZIP transcription factor B (*MAFB)*expression, a TF that interacts with Gcm2 and modulates parathyroid hormone, which in turn regulates Ca mass fraction [55]. These genes expressions were correlated to other six genes expression. Three of them were DEGs for Ca being part of pathways involved in ECM processes, and the other three were hub genes. From these hub genes, Bcl-2-modifying factor (*BMF)* regulates apoptosis after cell detachment from the ECM [56].

We identified the RAS like family 11 member A (*RASL11A)*, which encodes a RAS protein, with significant RIF for Cu. This gene expression was correlated mainly to the expression of genes involved in fatty acid metabolism, a process where Cu is a known enzymatic co-factor [57]. RAS proteins' posttranslational modifications are affected by fatty acids [58], possibly explaining the link of this gene expression with the fatty acid-related proteins.

For S, we identified Fucosyltransferase 8 (*FUT8)*, RAB44 member RAS oncogene family (*RAB44)*, Proline-rich and gla domain 3 (*PRRG3)*, Protein-lysine methyltransferase METTL21E (*METTL21E)*, and Phospholipid phosphatase related 5 (*PLPPR5)* genes with significant RIF, presenting their expression values correlated or being part of immune response and signal transduction pathways. Sulfur amino acids affect inflammatory aspects of the immune system [59]. Although there is no primary connection between *FUT8* and *RAB44* proteins and the immune system, these proteins contribute to tumor progression [60] [61], in which a robust immune response is involved [62]. *PRRG3* encodes a vitamin K-dependent transmembrane protein with a GLA domain, involved in coagulation factors [63], a process that is linked to the innate immune system [64]. Regarding signal transduction pathways, *METTL21E* was linked to signaling pathways in mouse siRNA experiments [65], and *PLPPR5* encodes a protein member of the phosphatidic acid phosphatase family, acting in phospholipase D mediating signaling [66]. The bta-miR-500, who presented a significant RIF for S is a known regulator of the genes whose mRNA levels were correlated to this miRNA in our analysis.

For Se, all enriched pathways were related to ECM interactions and protein digestion and absorption. For this mineral, we identified six annotated genes with significant RIF,

Thyrotroph embryonic factor (*TEF)*, Zn finger DBF-type containing 2 (*ZDBF2)*, Tetratricopeptide repeat domain 21 (*TTC21A)*, Histidyl-tRNA synthetase (*HARS)*, DTW domain containing 1 (*DTWD1)*, and Pyruvate dehydrogenase kinase 3 (*PDK3)*. *TEF* is a TF and a leucine zipper protein [67], whose family is required for the activation of DDRs receptors, essential to matrix remodeling [68]. *PDK3* encodes an enzyme responsible for the regulation of glucose metabolism, among many other functions, is related to ECM remodeling [69]. We could not find a link among *ZDBF2*, *HASR*, and *DTWD1* genes expression and Se or the enriched pathways. They are candidates for future studies regarding these potential relationships.

Regarding Zn, even without over-represented pathways, it is possible to infer that the six elements presenting significant RIF are putatively regulators of several correlated genes expressions and a few DEGs, as already discussed by *NOX1*. From the six genes with significant RIF, Membrane-bound transcription factor peptidase, site 2 gene (*MBTPS2)* is also a hub gene encoding an intramembrane Zn metalloprotease and *TNR* encodes an ECM glycoprotein. This information can lead to the assumption that ECM processes can also be associated to Zn amount, as they putatively do to most of the other minerals in study [9].

New application for PCIT and RIF algorithms

The first co-expression network, containing genes and miRNAs expressions correlated to the mass fraction of at least one mineral, is considered to be a correlation network among elements from two different sources: sequencing (mRNA-Seq and miRNA-Seq) and a measure referring to the trait of interest, the minerals` GEBVs. Originally, outputs from PCIT algorithm forms co-expression networks based on significant correlations between gene and miRNA expression levels. PCIT works in two steps: first, a partial correlation is calculated for every trio of genes/miRNAs based on the expression values of these elements in a specific set of samples, giving us the strength of the linear relationship between every two items, independent of the third one. In the end, PCIT calculates, for each trio of genes expression, the average ratio of partial to direct correlations. This value is set as the information theory threshold for significant associations, not the same for every analysis, specific for each trio [15]. Statistically, both steps can be used to test the correlation and the significance threshold of other genetic elements, if they vary in the population. Thus, there is no statistical impediment of using PCIT in the way proposed here, to detect genes and miRNAs whose expression values variate in our samples in correlation with the minerals`

GEBVs, as proposed here, since they already represent just the additive genetic effect of the traits [26].

The RIF algorithm was developed to calculate the impact of TFs over a selected list of genes through the expression values of genes and TFs across samples, in two contrasting groups for the studied phenotype (in our case, minerals). This impact factor is calculated in two ways (RIF 1 and RIF 2). RIF 1 gives high scores to TFs that are most differentially co-expressed, highly abundant, and with more expression difference between the groups. RIF 2 gives a high score to TFs for which the expression can predict better the abundance of DEGs [16]. Again, there is no impediment in the analytical methodology to use other genetic information, *e.g.*, GEBVs, since it variates in the population. In our application, we used genes and miRNAs with expression values correlated to at least one mineral in the place of TFs, and GEBVs were used instead of selected genes. In this case, RIF 1 gives a high score to the genes or miRNAs that are most differentially co-expressed, highly abundant and with more expression difference between the contrasting groups (mineral specific groups and score-based groups, separately) and RIF 2 to genes and miRNAs for which the expression can predict better the magnitude of the GEBVs. Together, both new applications can be used to predict genes and miRNAs expressions correlated to mineral mass fraction and to pinpoint which ones have a regulatory impact over mineral amount.

Conclusion

By using a modification of the PCIT/RIF methodology, we were able to predict regulatory elements related to the mineral amount of ten minerals, indicating over-represented pathways linked to the mass fraction of each mineral and putative regulators that are mineral specific. Our analyses corroborate the link between mineral amounts and the ECM processes, including a relationship with Zn not seen in our previous analysis. In our proposed approach, PCIT can be applied to predict the relationship between gene transcripts or miRNAs and phenotypes, in a genome-wide fashion. Similarly, RIF may predict the regulatory impact of mRNAs and miRNAs levels over phenotypes. This new approach can be applied for any phenotype that is of interest for genomic selection and livestock breeding.

Methods

Figure 5 contains a flowchart of the steps of our methodology.

Samples

The Ethical Committee of Embrapa Pecuária Sudeste (São Carlos, São Paulo, Brazil) approved all experimental and animal protocols (CEUA 01/2013). We used the GEBVs from mineral mass fraction [26] and the mRNA-Seq [10], and miRNA-Seq [70] data from 113 samples of *Longissimus thoracis* muscle from Nelore steers that are part of the population already described in previous differential expression analysis related to mineral amount [9] [10].

The animals forming our samples came from a Nelore steer population described elsewhere [26], [71]. In summary, all animals come from half-sibling families, generated by artificial insemination in two different farms, transferred to Embrapa Pecuária Sudeste (São Carlos, São Paulo, Brazil) and maintained in feedlot system with *ad libitum* feed and water access until slaughter, approximately 70 days after the start of the confinement, where the muscle sample collection was done.

Mineral mass fraction and genetic estimated breeding value (GEBV)

Calcium (Ca), copper (Cu), potassium (K), magnesium (Mg), sodium (Na), phosphorus (P), sulfur (S), selenium (Se), zinc (Zn) and iron (Fe) mass fractions were determined from lyophilized and microwave-assisted digested samples, such as described elsewhere [26]. Calcium, Cu, K, Mg, Na, P, S, Zn, and Fe were determined by inductively coupled plasma optical spectrometry (ICP OES, Vista Pro-CCD with a radial view, Varian, Mulgrave, Australia). Selenium was determined by inductively coupled plasma mass spectrometry (ICP-MS 820-MS, Varian, Mulgrave, Australia).

The estimation of the genetic breeding value (GEBVs) for all the minerals' amount was previously made [26] through a Bayesian model that considered birthplace, feedlot location and breeding season in the contemporary groups as fixed effects and age at slaughter as a linear covariate.

mRNA-Seq and miRNA-Seq sequencing and quality control

The total RNA extraction, quality control, and sequencing were described elsewhere [70]. In summary, total RNA from all the 113 samples was extracted using Trizol® (Life Technologies, Carlsbad, CA) and its integrity was evaluated in a Bioanalyzer 2100® (Agilent,

Santa Clara, CA, USA). Regarding the mRNA-Seq data, the library preparation was made with the TruSeq® sample preparation kit, and the paired-end sequencing [10] was made in an Illumina HiSeq 2500®. For the miRNA-Seq data, the library preparation was made with TruSeq® small RNA sample preparation kit, and the single-end sequencing [70] was made in a MiSeq sequencer.

As a quality control for the sequences, we filtered out reads with less than 65 bp and Phred Score less than 24 for the mRNA-Seq data, and the removal of reads with less than 18 bp and Phred Score less than 28 of the miRNA-Seq data were made using the Seqyclean software (http://sourceforge.net/projects/seqclean/files/).

The reads that passed the quality control were aligned to the reference bovine genome ARS-UCD 1.2 with the STAR v.2.5.4 software [72] for the mRNA-Seq data and with the mirDeep2 software [73] for the miRNA-Seq. The same software was used to the identification and quantification of transcripts and miRNAs, respectively, in raw counts.

Filtering, normalization and batch effect correction

After quality control, the mRNA-Seq and miRNA-Seq expression data were filtered separately to remove the transcripts and miRNA not expressed in at least 22 samples, or approximately 20% of the samples.

A first component analysis was performed for the mRNA-Seq expression data, with the NOISeq v.2.16.0 software [74] to visually verify the batch effect of the birthplace, feedlot location, breeding season, age at slaughter, slaughter group and a combination of sequencing flowcell and lane over the expression data. The data were normalized using the VST function from DESEq2 software [75], and the batch effect correction for the combination of sequencing flowcell and lane was made using the ARSyNseq function from the NOISeq v.2.16.0 software [74]. For the miRNA-Seq expression data, the procedure was the same, with the batch effect test only for the sequencing lane.

PCIT (Partial Correlation Coefficient with Information Theory) with mRNA, miRNA and phenotypes

A new application of the PCIT algorithm [15] was developed to test the correlation between the expression values of genes and miRNAs that passed the quality control filters and the GEBVs for ten minerals.

549 The original application of the algorithm is used to test the co-expression between
550 genes by correlation analysis between expression values [15]. In our application, we included
551 the GEBVs for each one of the ten minerals evaluated here for each sample in the algorithm
552 input with the gene and miRNA expression values (called PCIT general). Using this
553 approach, we estimated the correlations among all the elements. Among the significant
554 correlations, we selected only the genes and miRNAs with expression values correlated to the
555 GEBV of at least one mineral. Due to the low number of miRNAs identified compared to the
556 high number of genes, we did one more PCIT analysis only with miRNAs expression values
557 and the GEBVs (called PCIT miRNA). The results from these two PCITs analysis were
558 combined. In the end we had a list of elements (genes and miRNAs) with expression values
559 correlated to each mineral GEBV.
560
561 **RIF (regulatory impact factor)**
562
563 A new application of the RIF algorithm [16] was applied to obtain the predict
564 regulatory impact of the genes and miRNAs with expression values associated with a given
565 mineral on the amount of the same mineral, considering its GEBVs. The original application
566 of the algorithm was developed to determine the regulatory impact of TFs over selected genes
567 (targets) related to a given trait through their expression values analysis between contrasting
568 groups for the same trait [16]. In our approach, for each mineral, we used the genes and
569 miRNAs with expression values correlated to a mineral, from the previous PCIT analyses, as
570 elements to be tested as regulators and the mineral GEBV as the target.
571 We carried out 10 different analyses with the RIF algorithm [16], being one for each
572 mineral. As input, we used the GEBVs for the 30 contrasting samples for each mineral as
573 targets (15 representing samples with high mineral mass fraction and 15 with low mineral
574 mass fraction) and the expression values for the genes and miRNAs correlated to the same
575 mineral as elements to be tested. To select these contrasting groups we expanded the sample
576 selection based on GEBVs previously made [9] [10]. Genes and miRNAs with RIF I or II
577 results higher than |1.96| were considered as significant, as authors suggest [16].
578
579 **RIF for all minerals together**
580
581 To identify genes and miRNAs with significant impact factor in all minerals' mass
582 fraction together, we used the new application for the RIF algorithm [16] using the GEBV

583 from 30 contrasting samples forming two groups regarding the amount of the ten minerals as
584 targets and the expression values for the genes and miRNAs correlated to at least one mineral
585 as elements to be tested.
586 To select contrasting samples for all the minerals together, we ranked our samples
587 based on a score. To calculate this score for each sample, we performed a principal
588 component analysis (PCA) using the GEBVs for ten minerals for the 113 samples. From the
589 PC results, the score of each sample was calculated based on the following formula:
590

591 $$A_i = \sum_{j=i}^{10} k\, Contrib_{ijk} \times Z_{ijk} \times \%V_{PCj}$$

592
593 Where: A_i = *score* for the animal *i*, $\sum_{j=i}^{10} k$ = sum of all minerals k, in all the PCs *j* and in all
594 the animals *i*, $Contrib_{ijk}$ = contribution of the animal *i* in the PC *j* for the mineral *k*, Z_{ijk} =
595 standardized value (standard deviation one and mean zero) of the GEBV for the mineral *k* for
596 the animal *i* in the PC *j* and $\%V_{PCj}$ = eigenvalue of the PC *j*.
597 We performed a functional annotation analysis using DAVID 6.8 software [76] with
598 the genes presenting significant RIFs for the score, representing all minerals together.
599
600 **Genes and miRNAs correlated to minerals**
601
602 Significant correlations obtained from PCIT [15] analysis between genes or miRNAs
603 expressions and minerals were used to build a co-expression network with the Cytoscape
604 software [77]. We overlapped the gene list from our network with the genes previously
605 reported from our research group based on the same population evaluated here presenting
606 differentially expressed to at least one mineral [9] [10], TFs [17], affected by cis or trans
607 eQTLs [18] and with significant RIF. These features were used as attributes in the network.
608 Regarding the differentially expressed genes (DEGs) for Fe [10], we called the genes more
609 expressed in the high Fe content group as upregulated and the genes more expressed in the
610 low Fe content group as downregulated, to match the nomination of the other minerals'
611 DEGs [9]. Functional annotation analyses were made using DAVID 6.8 software [76].
612
613
614

615 **Integration with DEGs**

616

617 To estimate the relationship among the genes or miRNAs with expression values
618 correlated with minerals and the DEGs between contrasting groups for mineral concentration
619 previously detected [9], we made ten separately PCIT [15] analysis. In these analyses, the
620 PCIT algorithm was used as proposed initially [15] to test the correlations among the genes
621 and miRNAs with expression values correlated to each mineral, and the DEGs previously
622 detected for the same mineral [9] [10].
623 The significant correlations identified in each analysis was used to obtain co-
624 expression networks with the Cytoscape software [77]. The NetworkAnalyzer tool for the
625 Cytoscape software [77] was used to obtain the connectivity degree of each gene and miRNA
626 in the networks. This value was used to identify the hub genes/miRNAs from the average of
627 the connectivity degree from the network summed with the double of the referent standard
628 deviation.
629 We considered only the significant correlations containing at least a hub or significant
630 RIF gene/miRNA for a given mineral. The genes present in these considered correlations
631 were used to perform a functional annotation analysis with the STRING v.1.2.2 software
632 [78]. From these analyses, we selected the genes being part of enriched pathways considering
633 KEGG [79] and Reactome [19] databases with *Bos taurus* reference genome.
634

635 **Putative regulators of the genes being part of enriched pathways**

636

637 To identify the elements putatively regulating the genes being part of over-
638 represented pathways for each mineral in the study, we did another round of PCIT [15]
639 analyses, separately for each mineral. In this case, from each mineral last PCIT analysis, we
640 selected as inputs the genes being part of enriched pathways, also considering the previously
641 enriched pathways from differentially expressed genes related to mineral amount [9] [10], the
642 hub elements, TFs [17], miRNAs and the ones with significant RIFs, with their respective
643 attributes. The PCIT [15] results were used to obtain co-expression networks with Cytoscape
644 [77] software.
645
646
647
648

649 **miRNA-gene targeting confirmation**

650

651 We used TargetScan software [80] to predict the target genes for the miRNAs with
652 expression values correlated to a mineral in Figures 3 and 4 and we compared these putative
653 targets with the genes with expression values correlated to them in our networks.

654

655 **References**

656

657 [1] Geesink GH, Koohmaraie M. Effect of Calpastatin on Degradation of Myofibrillar
658 proteins by μ -Calpain Under Postmortem Conditions. J Anim Sci 1999; 77:2685–92.
659 [2] Williams P. Nutritional composition of red meat. Nutr Diet. 2007;64:S113-19.
660 [3] Doyle JJ, Spaulding JE. Toxic and Essential Trace Elements in Meat - a Review. J Anim
661 Sci. 1978;47(2):398–419.
662 [4] Campbell I. Macronutrients, minerals, vitamins and energy. Anaesth Intensive Care Med.
663 2017;18(3):141–6.
664 [5] Ahola JK, Baker DS, Burns PD, Mortimer RG, Enns RM, Whittier JC et al. Effect of copper,
665 zinc, and manganese supplementation and source on reproduction, mineral status, and
666 performance in grazing beef cattle over a two-year period. J. Anim. Sci. 2004**;** 95:2357-2383.
667 [6] Genther ON, Hansen SL. Effect of dietary trace mineral supplementation and a multi-
668 element trace mineral injection on shipping response and growth performance of beef cattle. J
669 Anim Sci. 2014;92(6):2522–30.
670 [7] Enjalbert F, Lebreton P, Salat O. Effects of copper, zinc and selenium status on
671 performance and health in commercial dairy and beef herds: Retrospective study. J Anim
672 Physiol Anim Nutr. 2006;90(11–12):459–66.
673 [8] Mateescu RG, Garmyn AJ, Tait JG, Duan Q, Liu Q, Mayes MS, et al. Genetic parameters
674 for concentrations of minerals in longissimus muscle and their associations with palatability
675 traits in angus cattle. J Anim Sci. 2013;91(3):1067–75.
676 [9] Afonso J, Coutinho LL, Tizioto PC, Diniz WJS, De Lima AO, Rocha MIP et al. Muscle
677 transcriptome analysis reveals genes and metabolic pathways related tomineral concentration
678 in *Bos indicus.* Sci Rep. 2019;9:1-11.
679 [10] Diniz WJ, Coutinho LL, Tizioto PC, Cesar ASM, Gromboni CF, Nogueira ARA, et al.
680 Iron content affects lipogenic gene expression in the muscle of Nelore beef cattle. PLoS One.
681 2016;11(8):1–19.
682 [11] Hudson NJ, Dalrymple BP, Reverter A. Beyond differential expression: the quest for

683 causal mutations and effector molecules. BMC Genomics. 2012;13(1):1-16.
684 [12] Serin EAR, Nijveen H, Hilhorst HWM, Ligterink W. Learning from Co-expression
685 Networks: Possibilities and Challenges. Front Plant Sci. 2016;7:1–18.
686 [13] Diniz WJS, Mazzoni G, Coutinho LL, Banerjee P, Geistlinger L, Cesar ASM, et al.
687 Detection of Co-expressed Pathway Modules Associated With Mineral Concentration and
688 Meat Quality in Nelore Cattle. Front Genet. 2019;10:1–12.
689 [14] Langfelder P, Horvath S. WGCNA: an R package for weighted correlation network
690 analysis. BMC Bioinformatics. 2008;9:1-13.
691 [15] Reverter A, Chan EKF. Combining partial correlation and an information theory
692 approach to the reversed engineering of gene co-expression networks. Bioinformatics.
693 2008;24(21):2491–7.
694 [16] Reverter A, Hudson NJ, Nagaraj SH, Pérez-Enciso M, Dalrymple BP. Regulatory impact
695 factors: Unraveling the transcriptional regulation of complex traits from expression data.
696 Bioinformatics. 2010;26(7):896–904.
697 [17] de Souza MM, Zerlotini A, Geistlinger L, Tizioto PC, Taylor JF, Rocha MIP, et al. A
698 comprehensive manually-curated compendium of bovine transcription factors. Sci Rep .
699 2018;8(1):1–12.
700 [18] Cesar ASM, Regitano LCA, Reecy JM, Poleti MD, Oliveira PSN, de Oliveira GB, et al.
701 Identification of putative regulatory regions and transcription factors associated with
702 intramuscular fat content traits. BMC Genomics. 2018;19(1):1–20.
703 [19] Fabregat A, Jupe S, Matthews L, Sidiropoulos K, Gillespie M, Garapati P, et al. The
704 Reactome Pathway Knowledgebase. Nucleic Acids Res. 2018;46:D649–55.
705 [20] Salazar G, Huang J, Feresin RG, Zhao Y, Griendling KK. Zinc regulates Nox1
706 expression through a NF-κB and mitochondrial ROS dependent mechanism to induce
707 senescence of vascular smooth muscle cells. Free Radic Biol Med. 2017;108:225–35.
708 [21] Brigelius-Flohé R, Kipp AP. Selenium in the redox regulation of the Nrf2 and the Wnt
709 pathway. Methods Enzymol. 2013;527:65–86.
710 [22] Maltzahn JV, Chang NC, Bentzinger CF, Rudnicki MA. Wnt signaling in myogenesis.
711 Trends in Cell Biol. 2012; 22:602-9.
712 [23] Park SH, Ryu SH, Suh PG, Kim H. Assignment of human PLCB2 encoding PLC β2 to
713 human chromosome 15q15 by fluorescence in situ hybridization. Cytogenet Genome Res.
714 1998;83(1–2):48–9.
715 [24] Seidman SA, Johnson NA, Arbelo U, Aribindi K, Bhattacharya SK. Tissue protein and
716 lipid alterations in response to metallic impaction. J Cell Biochem. 2019;120(2):2347–61.

[25] Behera R, Kothekar MD, Kale DS, Krishnamurthi K, Sirothia AR, Kalorey DR, et al. Study of mutations in aminolevulinic acid dehydratase (ALAD) gene in cattle from fly ash zone in Maharashtra, India. Indian J Anim Res. 2016;50(1):19–22.

[26] Tizioto PC, Taylor JF, Decker JE, Gromboni CF, Mudadu MA, Schnabel RD, et al. Detection of quantitative trait loci for mineral content of Nelore *longissimus dorsi* muscle. Genet Sel Evol. 2015;47(1):1–9.

[27] Itkin M, Heinig U, Tzfadia O, Bhide AJ, Shinde B, Cardenas PD, et al. Biosynthesis of antinutritional alkaloids in solanaceous crops is mediated by clustered genes. Science. 2013;341:175–9.

[28] Lanier LL, O'Fallon S, Somoza C, Phillips JH, Linsley PS, Okumura K, et al. CD80 (B7) and CD86 (B70) provide similar costimulatory signals for T cell proliferation, cytokine production, and generation of CTL. J Immunol. 1995;154(1):97–105.

[29] Lozanoska-Ochser B, Klein NJ, Huang GC, Alvarez RA, Peakman M. Expression of CD86 on Human Islet Endothelial Cells Facilitates T Cell Adhesion and Migration. J Immunol. 2008;181(9):6109–16.

[30] George AB, Kanellopoulou C, Masutani E, Chaigne-delalande B, Michael J. ITK is a magnesium sensor during T cell activation. J Immunol. 2017;198:1-10.

[31] Chandy KG, Wulff H, Beeton C, Pennington M, Gutman GA, Cahalan MD. K+ channels as targets for specific immunomodulation. Trends Pharmacol Sci. 2004;25(5):280–9.

[32] Gavile CM, Barwick BG, Newman S, Neri P, Nooka AK, Lonial S, et al. CD86 regulates myeloma cell survival. Blood Adv. 2017;1(25):2307–19.

[33] Ferrari S, Bonjour JP, Rizzoli R. The vitamin D receptor gene and calcium metabolism. Trends Endocrinol Metab. 1998;9(7):259–65.

[34] Uwitonze AM, Razzaque MS. Role of Magnesium in Vitamin D Activation and Function. J Am Osteopath Assoc. 2018;118(3):181-89.

[35] Harrington M, Bennett T, Jakobsen J, Ovesen L, Brot C, Flynn A, et al. The effect of a high-protein , high-sodium diet on calcium and bone metabolism in postmenopausal women and its interaction with vitamin D receptor genotype. Br J Nutr. 2004;25:41–51.

[36] Marcellini S, Bruna C, Henríquez JP, Albistur M, Reyes AE, Barriga EH, et al. Evolution of the interaction between Runx2 and VDR, two transcription factors involved in osteoblastogenesis. BMC Evol Biol. 2010;10(1):1–12.

[37] Mayr T, Deutsch U, Kühl M, Drexler HCA, Lottspeich F, Deutzmann R, et al. Fritz: A secreted frizzled-related protein that inhibits Wnt activity. Mech Dev. 1997;63(1):109–25.

751 [38] Yao L, Sun YT, Sun W, Xu TH, Ren C, Fan X, et al. High phosphorus level leads to
752 aortic calcification via β-catenin in chronic kidney disease. Am J Nephrol. 2015;41(1):28–36.
753 [39] Du J, Zu Y, Li J, Du S, Xu Y, Zhang L, et al. Extracellular matrix stiffness dictates Wnt
754 expression through integrin pathway. Sci Rep. 2016;6:1–12.
755 [40] Larriba MJ, González-Sancho JM, Barbáchano A, Niell N, Ferrer-Mayorga G, Muñoz A.
756 Vitamin D is a multilevel repressor of Wnt/β-catenin signaling in cancer cells. Cancers.
757 2013;5(4):1242–60.
758 [41] Guo S, Zhang W, Weia C, Wang L, Zhu G, Shi Q, et al. Serum and skin levels of miR-
759 369-3p in patients with psoriasis and their correlation with disease severity. Eur J
760 Dermatology. 2013;23(5):608–13.
761 [42] Regenhard P, Leippe M, Schubert S, Podschun R, Kalm E, Grötzinger J, et al.
762 Antimicrobial activity of bovine psoriasin. Vet Microbiol. 2009;136:335–40.
763 [43] Lowes MA, Bowcock AM, Krueger JG. Pathogenesis and therapy of psoriasis. Nature.
764 2007;445:866–73.
765 [44] Cubillos S, Norgauer J. Low Vitamin D-modulated calcium-regulating proteins in
766 psoriasis vulgaris plaques: S100A7 overexpression depends on joint involvement. Int J Mol
767 Med. 2016;38(4):1083–92.
768 [45] Kazandjieva J, Grozdev I, Darlenski R, Tsankov N. Climatotherapy of psoriasis. Clin
769 Dermatol. 2008;26(5):477–85.
770 [46] Senni K, Foucault-Bertaud A, Godeau G. Magnesium and connective tissue. Magnes
771 Res. 2003;16(1):70–4.
772 [47] Jabłońska-Trypuć A, Matejczyk M, Rosochacki S. Matrix metalloproteinases (MMPs),
773 the main extracellular matrix (ECM) enzymes in collagen degradation, as a target for
774 anticancer drugs. J Enzyme Inhib Med Chem. 2016;31:177–83.
775 [48] Yamamoto Y, Irie K, Kurihara H, Sakai T, Takai Y. Vmac: A novel protein associated
776 with vimentin-type intermediate filament in podocytes of rat kidney. Biochem Biophys Res
777 Commun. 2004;315(4):1120–5.
778 [49] Geiger B, Bershadsky A, Pankov R, Yamada KM, Correspondence BG. Transmembrane
779 Extarcelluler Matrix-Cytoskeleton. Nat Ver Mol Cell Biol. 2001;2:793-805.
780 [50] Graña X, Reddy EP. Cell cycle control in mammalian cells: role of cyclins, cyclin
781 dependent kinases (CDKs), growth suppressor genes and cyclin-dependent kinase inhibitors
782 (CKIs). Oncogene. 1995;11(2):211–9.
783 [51] Moreno-Layseca P, Streuli CH. Signalling pathways linking integrins with cell cycle
784 progression. Matrix Biol. 2014;34:144–53.

785 [52] Chauhan S, Titus DE, O'Brian MR. Metals control activity and expression of the heme
786 biosynthesis enzyme δ-aminolevulinic acid dehydratase in Bradyrhizobium japonicum. J
787 Bacteriol. 1997;179(17):5516–20.
788 [53] Bardag-Gorce F, French SW. Delta-aminolevulinic dehydratase is a proteasome
789 interacting protein. Exp Mol Pathol. 2011;91(2):485–9.
790 [54] Kammerl IE, Meiners S. Proteasome function shapes innate and adaptive immune
791 responses. Am J Physiol - Lung Cell Mol Physiol. 2016; 311:L328-36.
792 [55] Kamitani-Kawamoto A, Hamada M, Moriguchi T, Miyai M, Saji F, Hatamura I, et al.
793 MafB interacts with Gcm2 and regulates parathyroid hormone expression and parathyroid
794 development. J Bone Miner Res. 2011;26(10):2463–72.
795 [56] Delgado M, Tesfaigzi Y. Is BMF central for anoikis and autophagy ? Autophagy.
796 2014;10:1–2.
797 [57] Cunnane C. Differential regulation of essential fatty acid metabolism to the
798 prostaglandins: possible basis for the interaction of zinc and copper in biological systems.
799 Prog Lipid Res. 1982;21:73–90.
800 [58] Tamanoi F, Hsueh EC, Goodman LE, Cobitz AR, Detrick RJ, Brown WR, et al.
801 Posttranslational modification of ras proteins: Detection of a modification prior to fatty acid
802 acylation and cloning of a gene responsible for the modification. J Cell Biochem.
803 1988;36(3):261–73.
804 [59] Grimble RF. The effects of sulfur amino acid intake on immune function in humans. J
805 Nutr. 2006;136:1660S-1665S.
806 [60] Chen C-Y, Jan Y-H, Juan Y-H, Yang C-J, Huang M-S, Yu C-J, et al. Fucosyltransferase
807 8 as a functional regulator of nonsmall cell lung cancer. Proc Natl Acad Sci.
808 2013;110(2):630–5.
809 [61] Macaluso M, Russo G, Cinti C, Bazan V, Gebbia N, Russo A. Ras family genes: An
810 interesting link between cell cycle and cancer. J Cell Physiol. 2002;192(2):125–30.
811 [62] Whiteside TL. Immune responses to malignancies. J Allergy Clin Immunol.
812 2010;125:S272-S283.
813 [63] Cranenburg ECM, Schurgers LJ, Vermeer C. Vitamin K:Thecoagulationvitamin that
814 became omnipotent. J Thromb heamostasis. 2017;98:145–61.
815 [64] Delvaeye M, Conway EM. Coagulation and innate immune responses: Can we view
816 them separately? Blood. 2009;114(12):2367–74.
817 [65] Huang J, Hsu YH, Mo C, Abreu E, Kiel DP, Bonewald F et al. METTL21C is a potential
818 pleiotropic gene for osteoporosis and sarcopenia acting through the modulation of the NFκB

819 signaling pathway. J Bone Miner Res. 2014;29(7):1531–40.
820 [66] Billah MM. Phospholipase D and cell signaling. Curr Opin Immunol. 1993;5(1):114–23.
821 [67] Drolet DW, Scully KM, Simmons DM, Wegner M, Chu KT, Swanson LW, Rosenfeld
822 MG. TEF, a transcription factor expressed specifically in the anterior pituitary during
823 embryogenesis, defines a new class of leucine zipper proteins.Genes and Develo.
824 2009;5:1739–53.
825 [68] Noordeen NA, Carafoli F, Hohenester E, Horton MA, Leitinger B. A transmembrane
826 leucine zipper is required for activation of the dimeric receptor tyrosine kinase DDR1. J Biol
827 Chem. 2006;281(32):22744–51.
828 [69] Sullivan WJ, Mullen PJ, Schmid EW, Flores A, Momcilovic M, Sharpley MS, et al.
829 Extracellular Matrix Remodeling Regulates Glucose Metabolism through TXNIP
830 Destabilization. Cell. 2018;175(1):117-132
831 [70] Oliveira GB, Regitano LCA, Cesar ASM, Reecy JM, Degaki KY, Poleti MD et al.
832 Integrative analysis of microRNAs and mRNAs revealed regulation of composition and
833 metabolism in Nelore cattle. BMC Genomics. 2018;19(1):1–16.
834 [71] de Oliveira PSN, Cesar ASM, do Nascimento ML, Chaves AS, Tizioto PC, Tullio RR, et
835 al. Identification of genomic regions associated with feed efficiency in Nelore cattle. BMC
836 Genet. 2014;15:10.
837 [72] Dobin A, Davis CA, Schlesinger F, Drenkow J, Zaleski C, Jha S, et al. STAR: Ultrafast
838 universal RNA-seq aligner. Bioinformatics. 2013;29(1):15–21.
839 [73] Friedländer MR, MacKowiak SD, Li N, Chen W, Rajewsky N. MiRDeep2 accurately
840 identifies known and hundreds of novel microRNA genes in seven animal clades. Nucleic
841 Acids Res. 2012;40(1):37–52.
842 [74] Tarazona S, Furió-Tarí P, Turrà D, Di Pietro A, Nueda MJ, Ferrer A, et al. Data quality
843 aware analysis of differential expression in RNA-seq with NOISeq R/Bioc package. Nucleic
844 Acids Res. 2015;43(21):15.
845 [75] Love MI, Huber W, Anders S. Moderated estimation of fold change and dispersion for
846 RNA-seq data with DESeq2. Genome Biol. 2014;15(12):15.
847 [76] Huang DW, Sherman BT, Lempicki RA. Systematic and integrative analysis of large
848 gene lists using DAVID bioinformatics resources. Nat Protoc. 2009;4(1):44–57.
849 [77] Shannon P, Markiel A, Ozier O, Baliga NS, Wang JT, Ramage D et al. Cytoscape: a
850 software environment for integrated models of biomolecular interaction networks. Genome
851 Res. 2003;13:2498–504.
852 [78] Pertea M, Pertea GM, Antonescu CM, Chang TC, Mendell JT, Salzberg SL. StringTie

enables improved reconstruction of a transcriptome from RNA-seq reads. Nat Biotechnol. 2015;33(3):290–5.

[79] Kanehisa M, Furumichi M, Tanabe M, Sato Y, Morishima K. KEGG: New perspectives on genomes, pathways, diseases and drugs. Nucleic Acids Res. 2017;45:D353–61.

[80] Agarwal V, Bell GW, Nam J-W, Bartel DP. Predicting effective microRNA target sites in mammalian mRNAs. Elife. 2015;4:1–38.

Acknowledgements

We thank FAPESP (2012/23638-8) for financing the projects encompassing this one and Capes for the scholarship for the first author. We thank all the Staff of Embrapa Pecuária Sudeste responsible for monitoring and taking care of animals. We thank CNPq for the productivity scholarship for the ninth, tenth and last authors. We also thank The University of Queensland for receiving the first author in a Ph.D. internship and the Commonwealth Scientific and Industrial Research Organisation (CSIRO) for assistance during the same internship.

Authors Contribution

J.A., M.R.S.F., A.R and L.C.A.R. designed the experiments and analysis. J.A., M.R.S.F., A.R., W.J.S.D., A.S.M.C, A.O.L., J.P., M.M.S., L.L.C., G.B.M., A.Z., C.F.G., A.R.A.N., performed the experiments and analysis. J.A., M.R.S.F., A.R. and L.C.A.R. interpreted the results. J.A. and M.R.S.F. drafted the manuscript. All authors revised and approved the final manuscript.

Competing Interests

The authors claim no competing interests.

887 **Table 1. Number of genes and miRNAs with expression values correlated to each**
888 **mineral considering both PCIT analysis.** PCIT general, with mineral genomic estimates of
889 breeding values, genes and miRNAs expression and PCIT miRNA with mineral GEBVs and
890 miRNAs expression. The data came from *Longissimus thoracis* muscle from Nelore steers
891 and the genes and miRNA expressions were identified based on RNA-Seq analysis.
892

Mineral	Gene	miRNA	Repeated miRNA[a]
Ca	22	6	0
Cu	35	5	0
K	33	5	0
Mg	37	8	0
Na	42	6	3
P	19	6	0
S	55	6	1
Se	32	6	2
Zn	36	9	0
Fe	27	5	1

893 [a] number of miRNAs with expression values correlated to a mineral in both PCIT analysis
894 (PCIT general and PCIT miRNA)
895
896
897 **Table 2. Number of genes and miRNAs with a significant regulatory impact factor over**
898 **the genomic estimates of breeding values for each mineral and all minerals together**
899 **(PCA score).** The data came from *Longissimus thoracis* muscle from Nelore steers and the
900 genes and miRNA expressions were identified based on RNA-Seq analysis.
901

Mineral	Gene	miRNA
Ca	1	1
Cu	4	0
K	3	1
Mg	3	1
Na	6	1
P	1	0
S	5	2
Se	7	0
Zn	4	2
Fe	0	2
PCA Score	22	2

902

Table 3. Number of genes and miRNAs with expression values correlated per mineral and per attribute considering both PCIT analysis. PCIT general, with mineral genomic estimates of breeding values, genes and miRNAs expression and PCIT miRNA with mineral GEBVs and miRNAs expression. The data came from *Longissimus thoracis* muscle from Nelore steers and the genes and miRNA expressions were identified based on RNA-Seq analysis. Attributes: a) differentially expressed genes [9] [10], b) genes and miRNAs with significant regulatory impact factor, c) transcription factors [17], d) genes affected by cis eQTLs [18], e) genes affected by trans eQTLs [18], f) miRNAs and g) genes and miRNAs with expression values correlated to each mineral that were not identified in previous works.

Minerals	DEGs[a]	Significant RIF[b]	TFs[c]	cis eQTLs[d]	trans eQTLs[e]	miRNAs[f]	No attributes[g]
Ca	0	3	2	0	3	5	14
Cu	1	4	1	0	1	5	28
K	2	5	2	0	7	3	19
Mg	2	6	2	0	5	6	23
Na	3	7	2	0	13	6	21
P	0	1	2	0	3	6	12
S	1	8	3	0	8	6	34
Se	1	9	2	1	3	6	17
Zn	0	6	1	0	3	9	27
Fe	3	19	0	0	2	5	9

Table 4. Pathways enriched for each mineral considering the gene expressions correlated to each one of them and the previously detected differentially expressed genes related to the same minerals in the same Nelore population. Pathways just enriched in previous works with a differential expression approach and the same Nelore population are marked in dark grey, pathways enriched in our correlated genes expressions are marked in black and the pathways enriched in both in previous work and in the correlated genes expressions are marked in light grey. There were no enriched pathways for Zn.

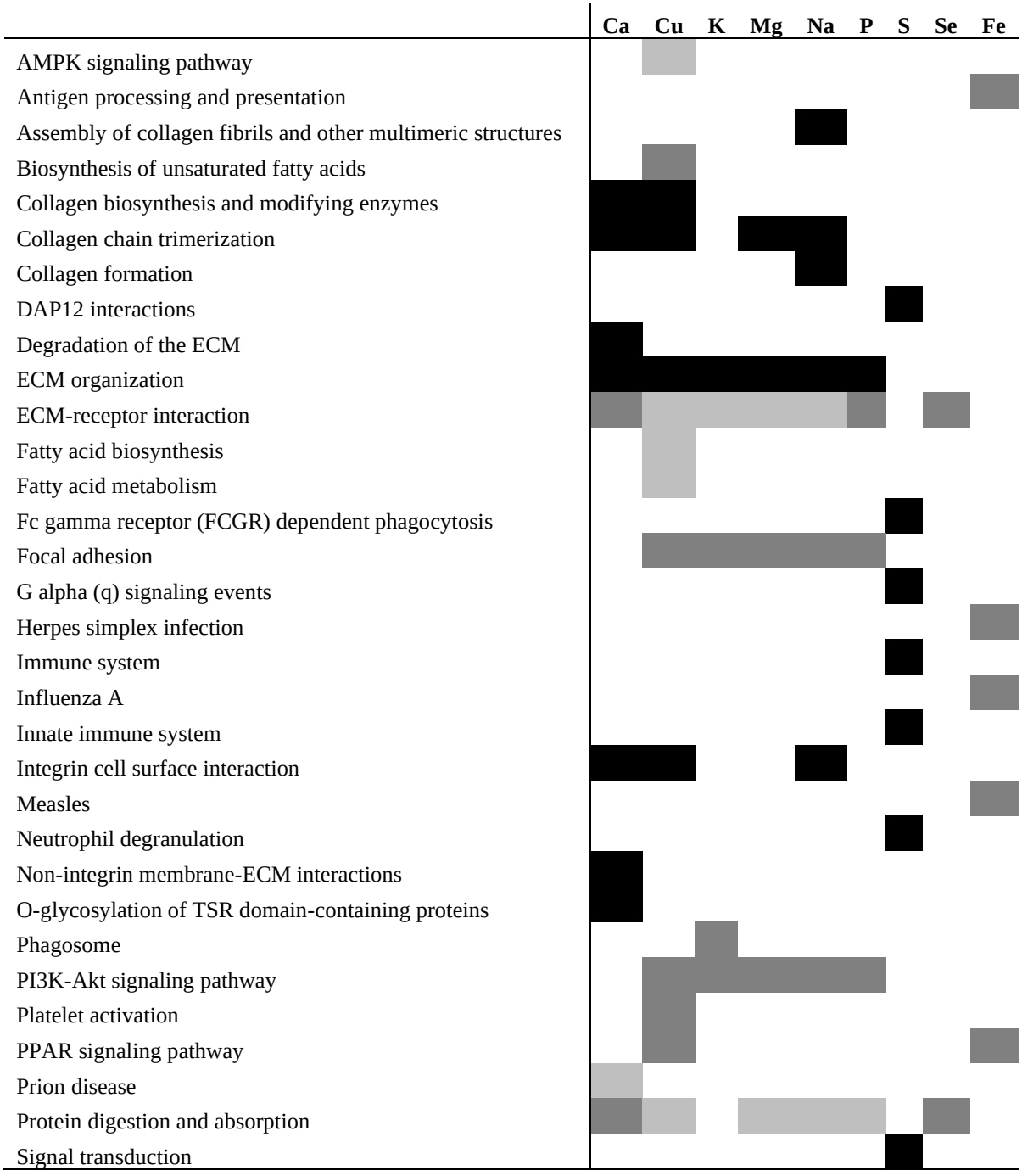

Figure 1. Co-expression network among genes and miRNAs with expression values correlated to at least one mineral. A) Complete network, B) Details about the correlations regarding the genes and miRNAs with expression values correlated to more than one mineral, the internal circle of the complete network, C) Correlations among the mineral's GEBVs.

A)

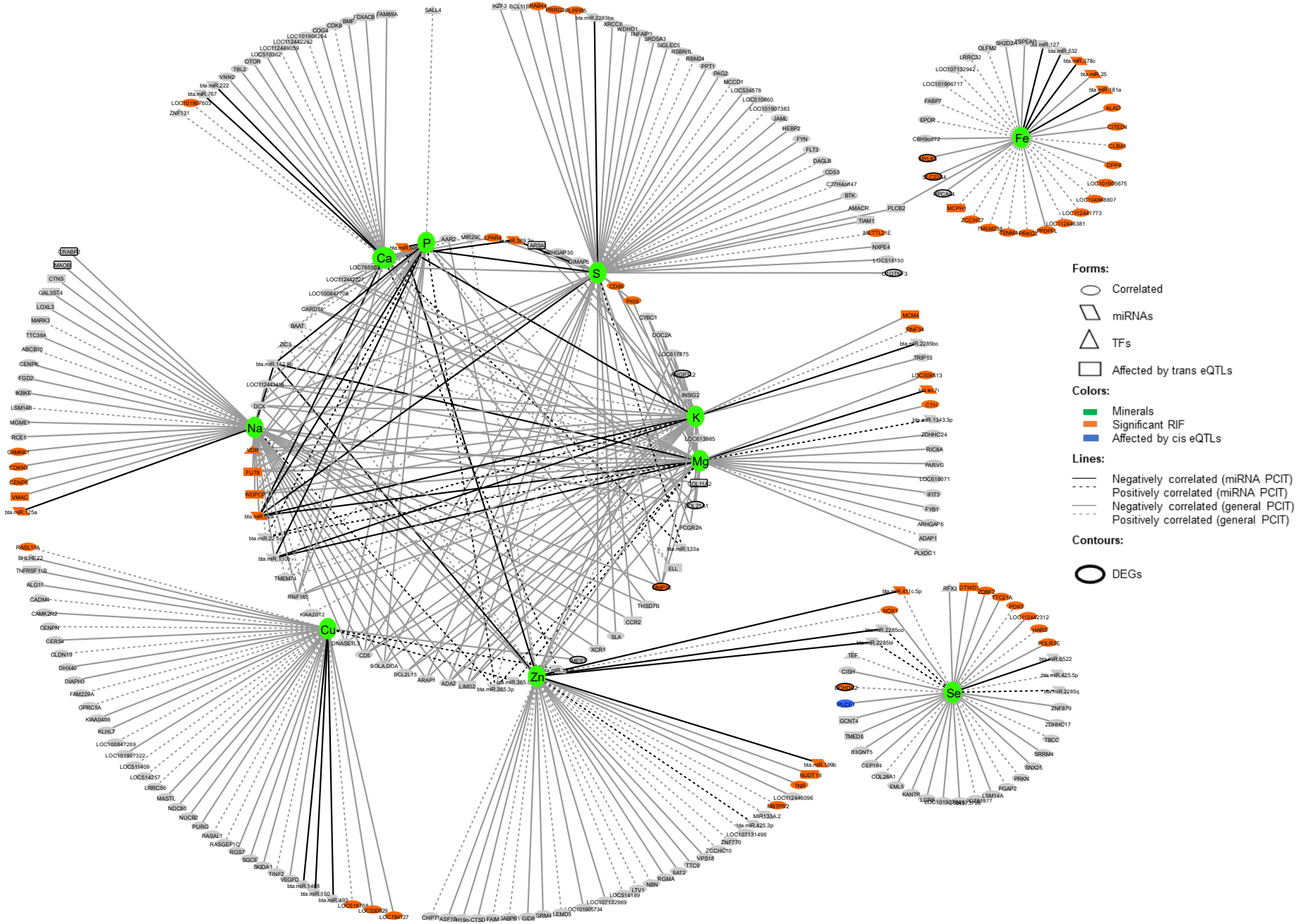
Ca
P
S
Fe
Na
K
Mg
Cu
Zn
Se
Forms:
Correlated
miRNAs
TFs
Affected by trans eQTLs
Colors:
Minerals
Significant RIF
Affected by cis eQTLs
Lines:
Negatively correlated (miRNA PCIT)
Positively correlated (miRNA PCIT)
Negatively correlated (general PCIT)
Positively correlated (general PCIT)
Contours:
DEGs

B)

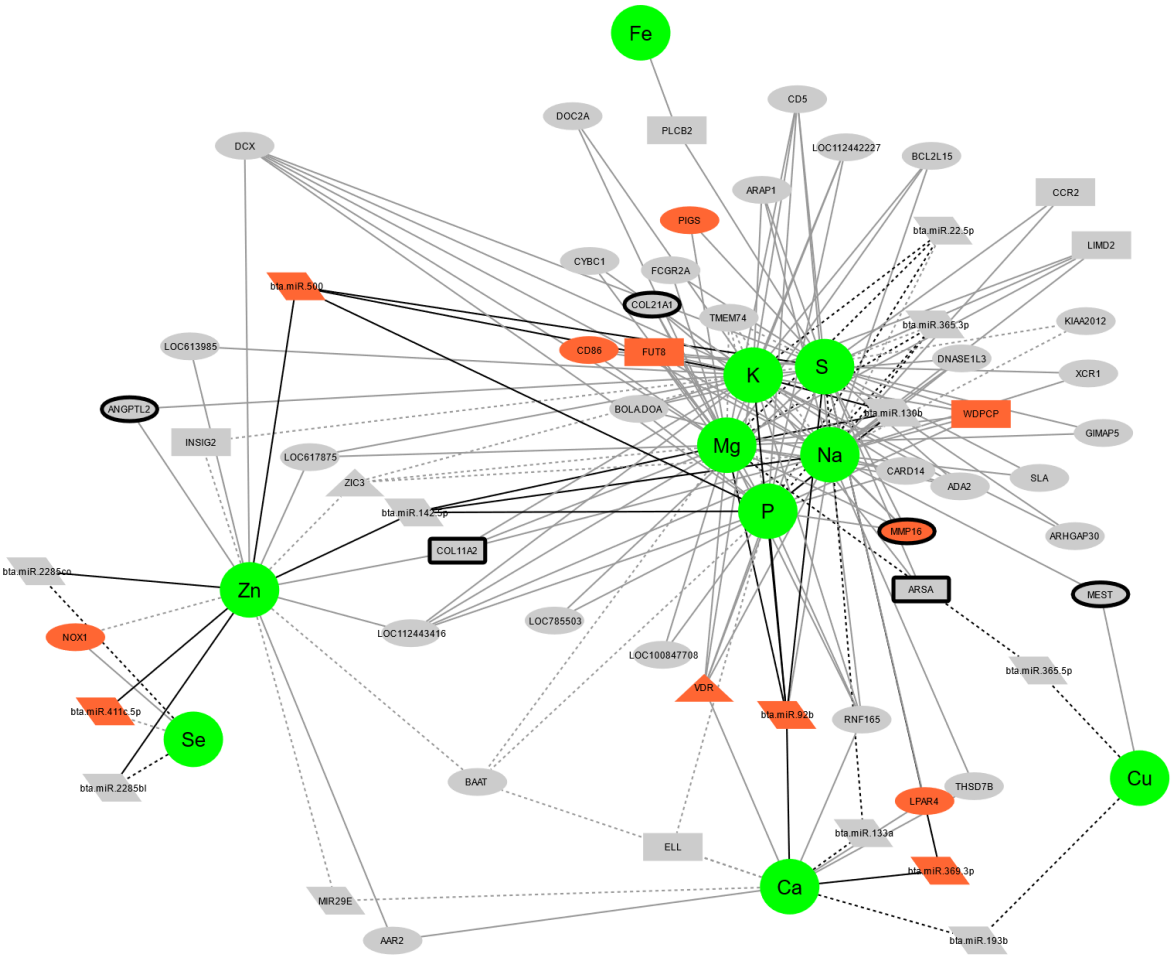

C)

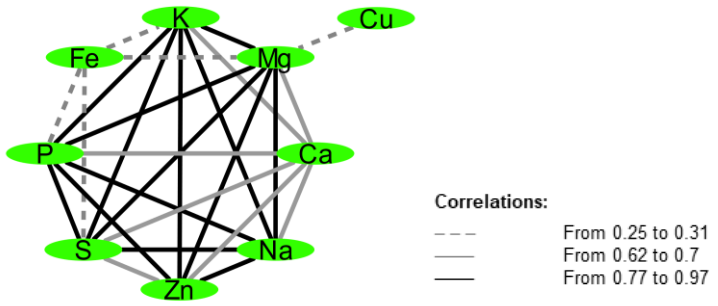

Figure 2. Representation of the contrasting samples considering the genomic estimated breeding values of all 10 minerals together, based on the PCA score. Orange circles represent the samples with the highest scores (positive contrast) and the green circles represent the samples with the lowest scores (negative contrast).

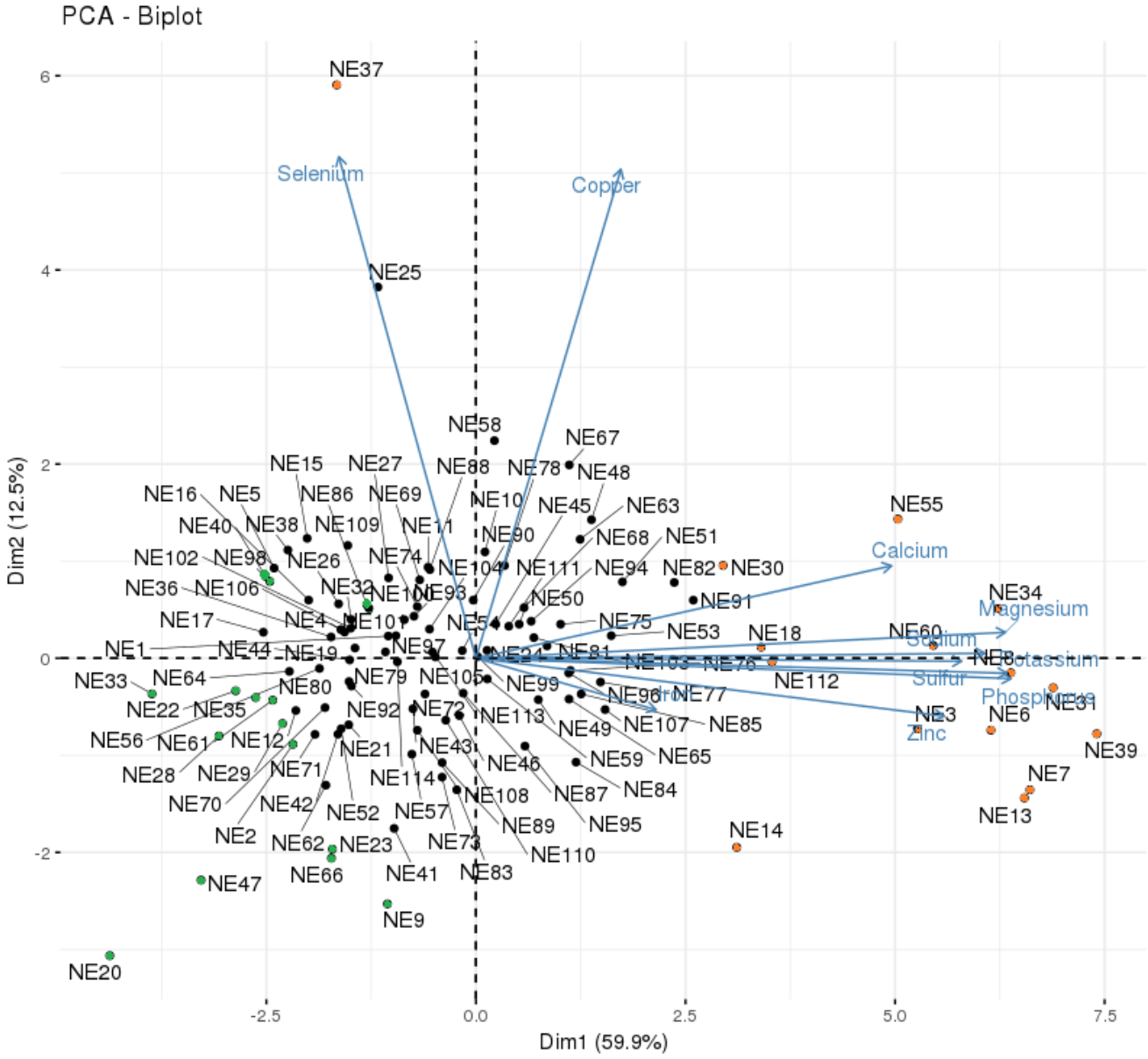

Figure 3. Co-expression networks among genes and miRNAs being part of enriched pathways (DEGs and correlated to a mineral), hubs, TFs, miRNAs or presenting a significant RIF regarding nine of the minerals in study. A) Mg, B) Fe, C) Ca, D) Se, E) K, F) Na, G) Cu, H) P, I) S. Red lines represent the correlations with a significant RIF gene or miRNA.

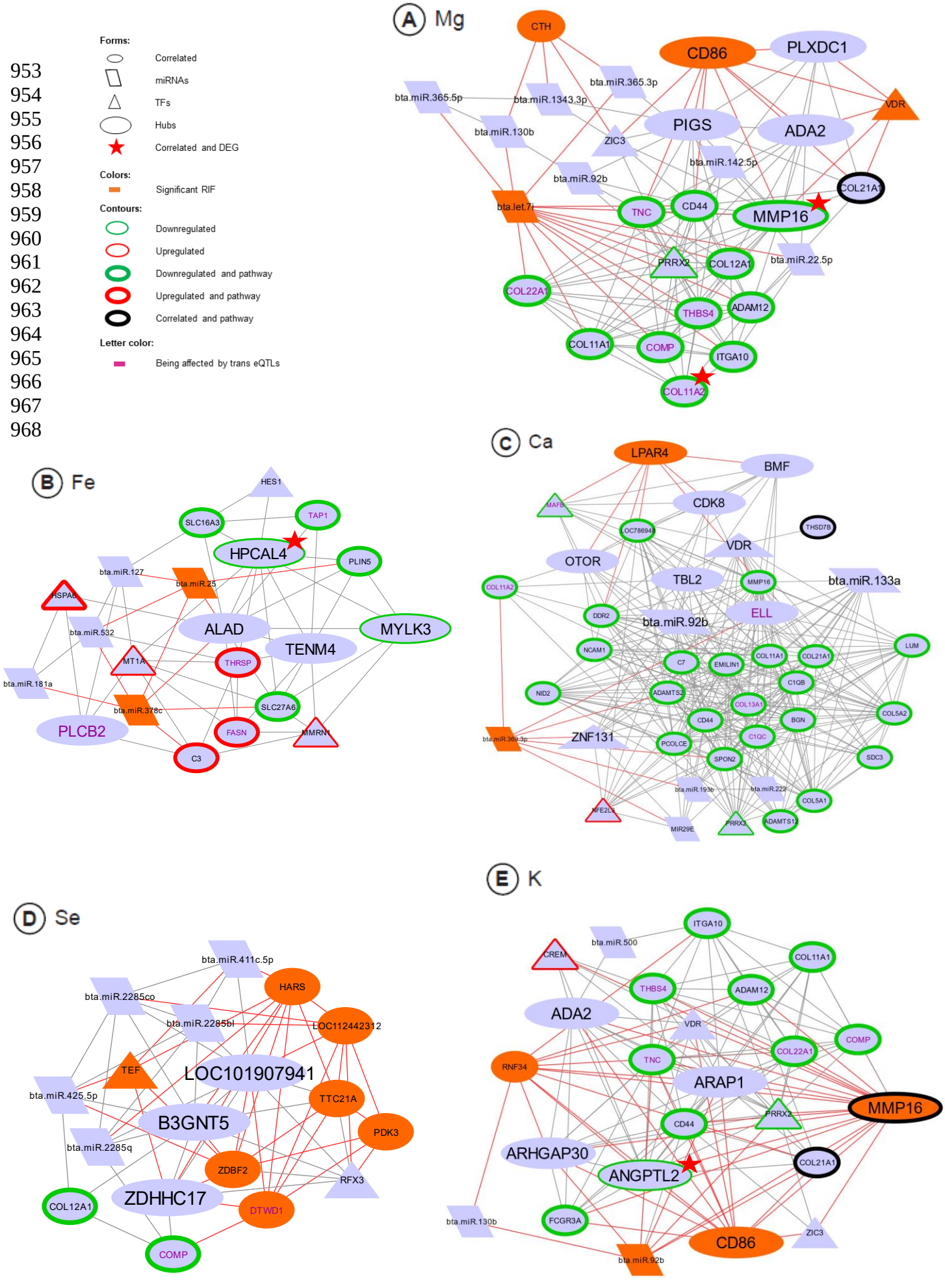

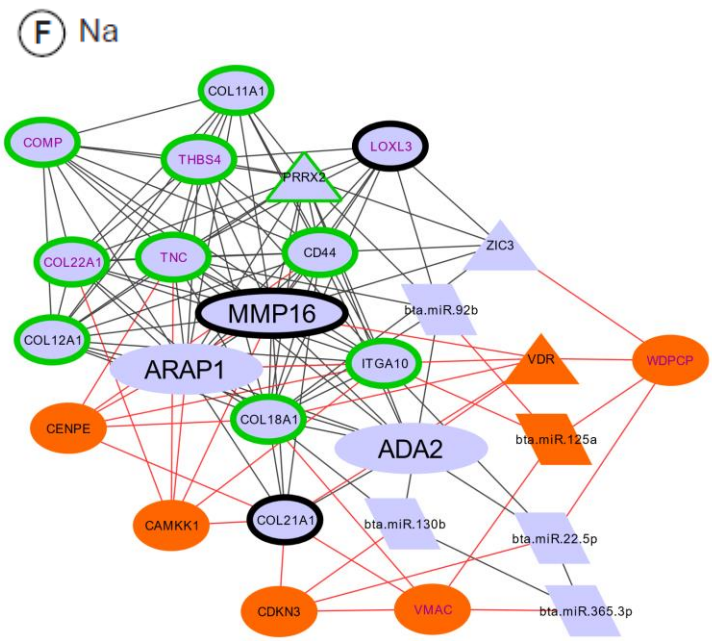

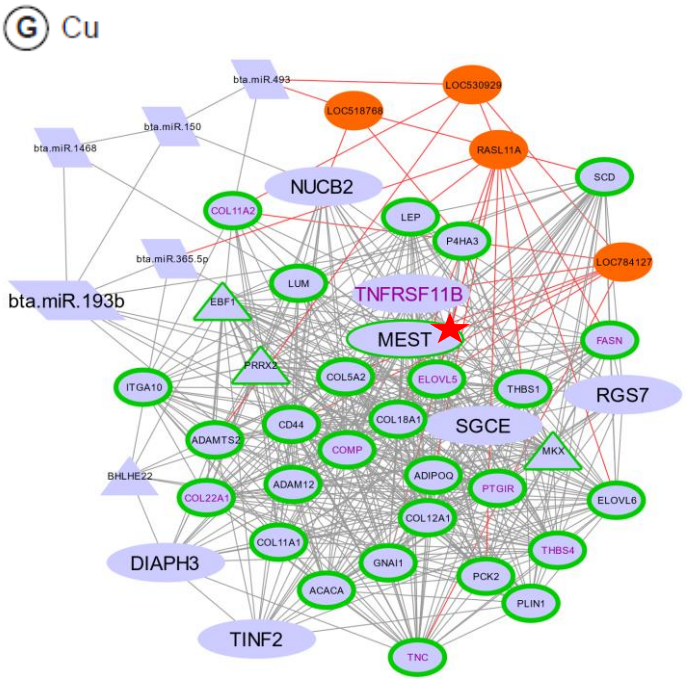

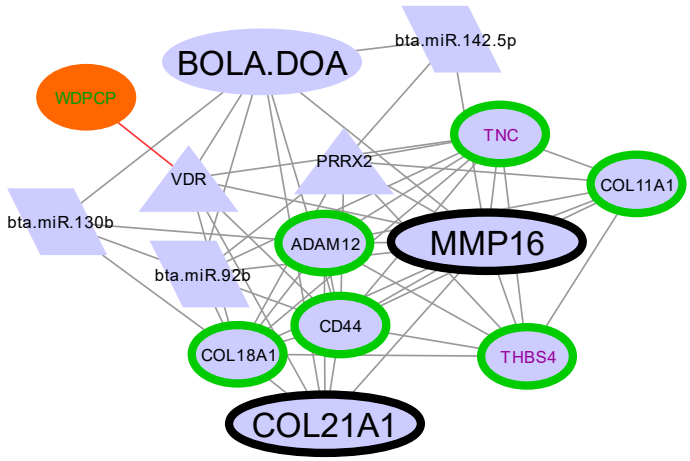

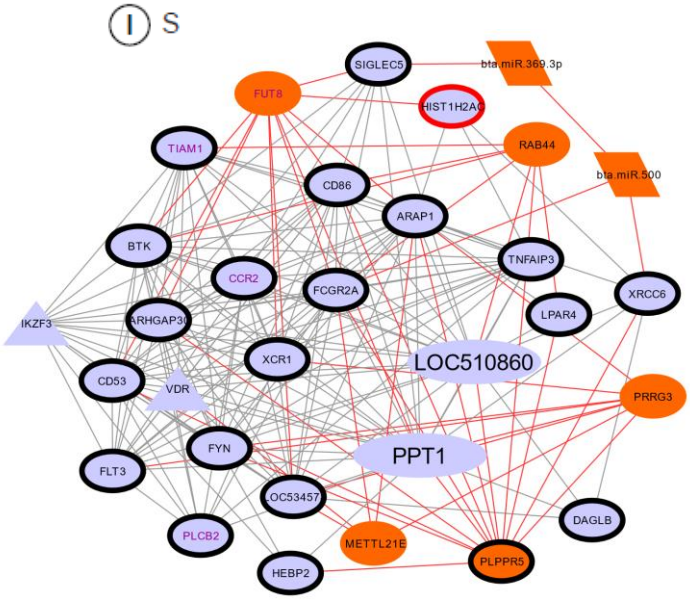

Figure 4. Co-expression network containing DEGs for Zn, genes or miRNAs with expression values that are correlated to these DEGs and are also a hub or a significant RIF for Zn, ora miRNA correlated to Zn. Their functional attributes are presented in different colors or shapes. Red lines represent the correlations with a significant RIF gene or miRNA.

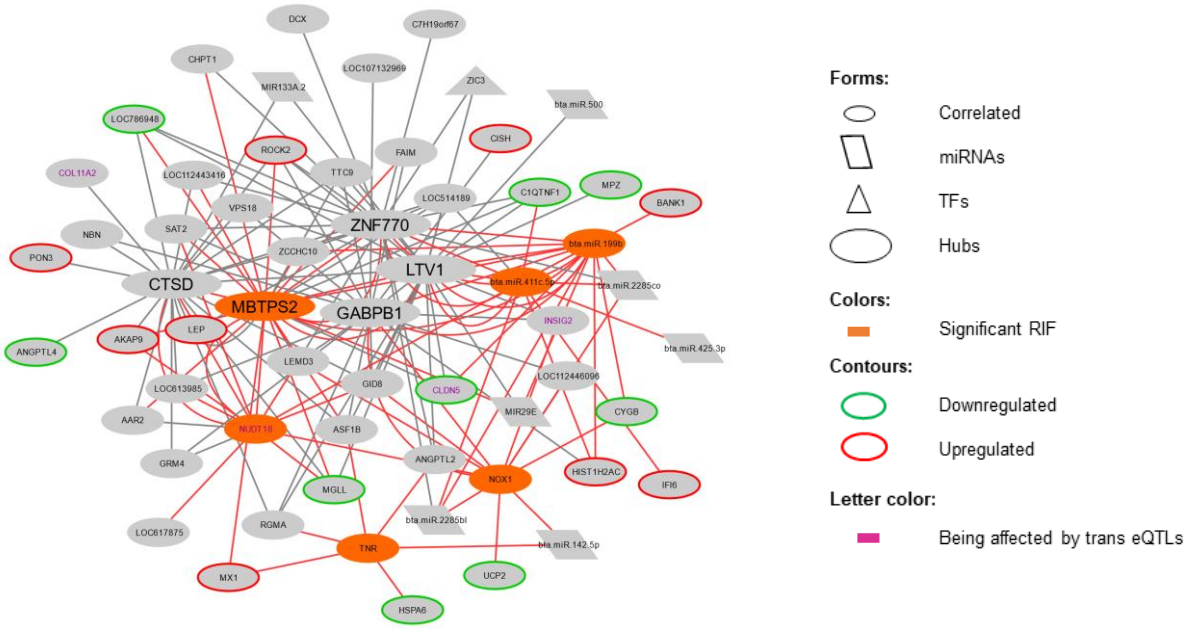

Figure 5. Flowchart representing the steps of the methodology.